Journal of Materials Chemistry C

ROYAL SOCIETY OF CHEMISTRY

PAPER

View Article Online
View Journal | View Issue

Cite this: J. Mater. Chem. C, 2023, 11, 4929

Constructing high-performance low-temperature curable PI materials by manipulating the side group effects of diamine†

Shan Huang,‡[ab] Xialei Lv,‡[a] Yao Zhang,[a] Jinhui Li,*[a] Shilu Zhou,[a] Siyao Qiu,[a] Zimeng He,[a] Tao Wang,[a] Guoping Zhang*[a] and Rong Sun[a]

To date, low-temperature curable polyimide (PI) materials have been in great demand in the field of advanced packaging. However, their synthesis is still a challenge due to the distinct structural design contradiction between the low-temperature curing ability and other desired properties. In this work, we designed and synthesized two novel diamines with different side groups (phenyl and pyrimidine rings), named $PhNH_2$ and $SPMNH_2$, and applied them to construct high-performance PI. Inspired by our previously reported pyrimidine based diamine $PMNH_2$ (X. Lv, S. Qiu, S. Huang, K. Wang and J. Li, *Polymer*, 2022, **261**, 125418), we tried to explore the impact of nitrogen heterocycle position (in the side group or main chain) on low-temperature curing ability. Compared with the typical diamine complex with nitrogen heterocycles in the main skeleton, the well-designed pyrimidine side group endowed the PI films with a highly improved imidization degree (ID) and excellent thermal and mechanical properties at a low curing temperature (200 °C). It should be noted that the configurations and the side group effects of diamine could modulate the temperature of polymerization and the structure of polymers, which further influenced the final performance of PI films. The copolyimide films based on $SPMNH_2$ exhibited a high elongation of 103.4%, Young's modulus of 3.20 GPa, tensile strength of 147 MPa, 5wt % decomposition temperature ($T_{d5\%}$) of 524 °C, and a glass transition temperature (T_g) of 359 °C, which was much better than that for PI film copolymerization with $PhNH_2$ or $PMNH_2$ cured at 200 °C. Experimental results and theoretical calculations showed that the introduction of pyrimidine side groups allowed for a better catalytic effect in the reaction system, and stronger intermolecular force between the polymer chains. This is the first report about the side-group effects on low-temperature curable PI films, which should be enlightening for the design of novel and high-performance diamines applied for advanced packaging and other fields.

Received 17th January 2023,
Accepted 7th March 2023

DOI: 10.1039/d3tc00198a

rsc.li/materials-c

Introduction

With the development of the integrated circuit industry, polyimide (PI) has been extensively applied in the microelectronics field for its outstanding properties.[1–4] Traditional polyimide needs to be heat cured above 350 °C to ensure excellent performances, which limits its application in some processes of semiconductor manufacturing.[5–7] For example, the fan-out wafer level package (FOWLP) has attracted widespread attention from researchers and industries due to its low-cost and high I/O courts.[8] PI serves as the pivotal redistribution layer (RDL) of FOWLP, yet it is required to be cured below 250 °C to avoid wafer warpage and improve the reliability.[9–11] As such, the low-temperature curable PI materials are expected to possess suitable properties for specific practical application scenarios, for instance, junction materials for transistors, directional film materials for liquid crystal displays, and cover materials for tape automatic bonding. In this regard, incorporating low-temperature curing ability and good thermal/mechanical properties is an urgent demand in the field of semiconductor packaging.

According to previous research studies,[12–17] it is clear that designing new monomers is currently the most promising method to obtain low-temperature curable polyimide at low cost. In general, the monomers with flexible structures or nitrogen heterocycles are designed to prepare low-temperature curable

[a] Shenzhen International Innovation Institutes of Advanced Electronic Materials, Shenzhen Institutes of Advanced Technology, Chinese Academy of Sciences, Shenzhen, 518055, China. E-mail: jh.li@siat.ac.cn, gp.zhang@siat.ac.cn
[b] Department of Nano Science and Technology Institute, University of Science and Technology of China, Suzhou, 215123, China

† Electronic supplementary information (ESI) available. See DOI: https://doi.org/10.1039/d3tc00198a

‡ These authors contributed equally to this work.

polyimide. The flexible structures improve the mobility of the molecular chains and reduce the interaction between polymer chains, which facilitates the lowering of the curing temperature of the polyimide.[16–19] Leu *et al.* introduced flexible groups and a large side group naphthalene in the monomer to increase the chain activity and break the conjugated system of the molecular backbone, which effectively reduced the curing temperature to 180 °C.[16] Besides, the nitrogen heterocycle could increase the nucleophilicity of diamines to attack carbonyl carbon, facilitate the acylation reaction and decrease the curing temperature as reported.[20–24] Artem'eva *et al.* investigated the catalytic action of the pyrimidine fragments in the process of imidization, and they considered that there were two influences of the pyrimidine ring on thermal curing: (1) the energy barrier of imidization might be decreased by this ring and (2) the pyrimidine ring could be conducive to more rapid and complete resynthesis of polyamide acid partly damaged by thermocyclization.[20] Subsequently, Li *et al.* reported pyrazine based diamine, and prepared a series of low-temperature curable PI films with an ID of about 73.1% when curing at 200 °C.[21] Sui *et al.* introduced 5-aminobenzimidazole as the terminal group to lower the curing temperature of PI films, which realized a high ID, and obtained PI films with tensile strength 93 MPa and elongation 15% at 200 °C.[22] These reports confirmed the effectiveness of nitrogen heterocycles in lowering the curing temperature of polyimide. However, few researchers have studied the effect of substitution sites of nitrogen heterocycles on reducing the curing temperature of polyimide until now.

In this work, we designed two new diamines with different side groups (phenyl and pyrimidine rings), named 4,4′-([1,1′-biphenyl]-2,4-diylbis(oxy))dianiline ($PhNH_2$) and 4,4′-((4-(pyrimidin-5-yl)-1,3-phenylene)bis(oxy))dianiline 4,4′-((4-(pyrimidin-5-yl)-1,3-phenylene)bis(oxy))dianiline ($SPMNH_2$), and used a diamine containing pyrimidine ring without side groups named 4,4′-(pyrimidine-2,4-diylbis(oxy))dianiline ($PMNH_2$), which was reported in our previous research as a contrast compound.[25] Serving as side groups, pyrimidine rings may approach the reactive centers (the amido acid fragments) more easily and thus provide better catalytic function at a lower curing temperature. Moreover, the bulky side group phenyl has a certain impact on reducing the curing temperature, whereas $PhNH_2$ showed an ID of 97.6% at 200 °C curing temperature. In addition, the pyrimidine ring present in the side group could be bound to the amido acid fragments of neighboring chains by hydrogen bonds and further increase the intermolecular interaction in copolymer polyimide (co-PI) films compared to the pyrimidine rings situated in the main chain. Above all, this work presented a new strategy for the structural design of diamine monomers and investigated the positional effect of pyrimidine units in diamines on reducing the curing temperature of polyimide, which further enriched the available material systems applied in the microelectronics industry.

Results and discussion

Synthesis and characterization of monomers

The designed monomers of $PhNH_2$ and $SPMNH_2$ were synthesized by the nucleophilic aromatic substitution reaction, Suzuki–Miyaura reaction and reduction reaction as shown in Scheme S1 (ESI†). The synthetic yields were beyond 80% and the intermediates and end products were confirmed by nuclear magnetic resonance (NMR) and high-resolution mass spectrometry (HRMS) as described in the ESI† (see Fig. S1–S8). High-performance liquid chromatography (HPLC) was also performed to estimate the purity of $PhNH_2$ and $SPMNH_2$ as shown in Fig. S9 (ESI†) and their purity was beyond 97%. In this work, we used a two-step thermal imidization procedure to prepare all PI films as described in the experimental part and their

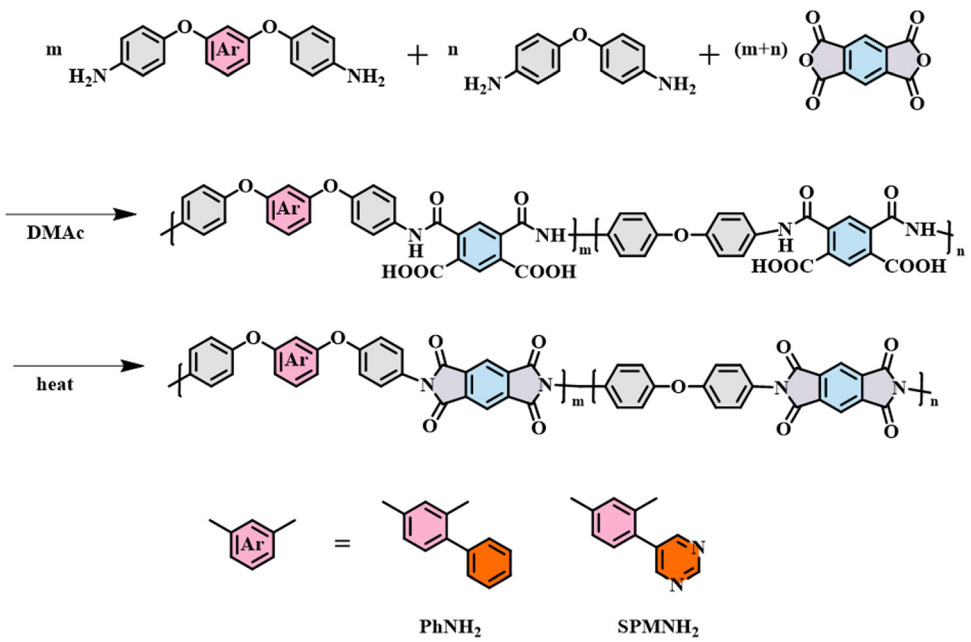

Fig. 1 Synthesis routes of the co-PI films.

synthesis routes are depictured in Fig. 1. The molecular weight of the resulting polyamide acid (PAA) was tested by gel permeation chromatography (GPC) as seen in Table S1 (ESI†), and all PAA solutions showed suitable M_n above 60 000 Da, which indicated the reasonability of the polymerization conditions.

Infrared analysis and XRD patterns

The FTIR spectra of the co-PI films are shown in Fig. 2 and Fig. S10 (ESI†). The co-PI films cured at 200 °C exhibited characteristic absorption bands near 1780 cm^{-1} (C═O asymmetric stretching of imide rings), 1720 cm^{-1} (C═O symmetric stretching of imide rings), 1380 cm^{-1} (N–C–N of imide rings) and 725 cm^{-1} (imide ring deformation). According to the reported methods,[26–28] the degree of imidization (ID) was calculated from the integral area of the four characteristic peaks of the imide ring mentioned above and the benzene ring as an internal standard at 200 °C and 350 °C, and the variation trend of IDs with the change in doping ratios is shown in Fig. 2c and d. Increased IDs were observed for co-PI films compared to the control sample PI-200 (ID_{1380} = 86.9%), suggesting that the introduction of bulky side groups (phenyl and pyrimidine rings) affected molecular chain movement, and contributed to lowering of the curing temperature of PI films. However, the IDs of ($PhNH_2$/ODA)/PMDA co-PI films showed a decreasing trend from 10 wt%. This result indicated that excessive bulky side groups would impede the movement of molecular chains,[29,30] which might be detrimental to the imidization process. Similarly, PI-$SPM_{10\%}$-200 had the highest ID_{1380} of 98.3%, and the IDs also exhibited first an increasing trend and then a decreasing trend with the additives $SPMNH_2$. This manifested that it was a battle between the nitrogen heterocycles of $SPMNH_2$ promoting the process of thermal imidization and excessive bulky side groups reducing the motility of molecular chains. Moreover, the same proportion of $SPMNH_2$ had higher ID compared to that of $PMNH_2$ (ID_{1380} = 92.8%), demonstrating that the pyrimidine side group was more conducive to lower curing temperature.

To further analyse the packing states of the molecular chains, the XRD patterns of co-PI films were measured and are illustrated in Fig. 3 and Fig. S11 (ESI†). The broad diffraction peaks of 2θ of PI-200 were located near 19°, indicating its amorphous nature. According to Bragg's law, the *d*-spacing values between the molecular chains were estimated (see Table 1 and Table S2, ESI†). Low-temperature curable co-PI films with $PhNH_2$ or $SPMNH_2$ showed larger *d*-spacing values compared to PI-200 due to the increased free volume of the molecular chains derived from the side groups. However, the *d*-spacing values of ($SPMNH_2$/ODA)/PMDA co-PI films were smaller than those of ($PhNH_2$/ODA)/PMDA co-PI films, confirming that the pyrimidine ring generated more hydrogen bonding between molecular chains and facilitated the formation of the imide ring. Moreover, although $PMNH_2$ did not

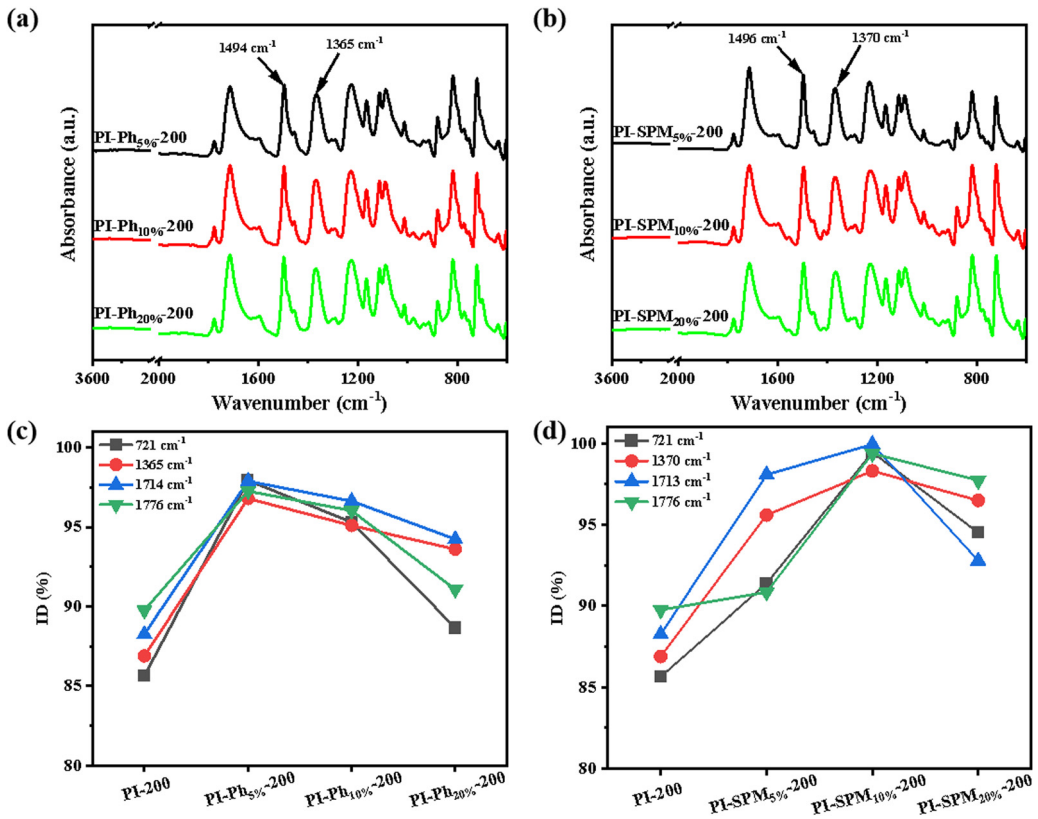

Fig. 2 FTIR spectra of (a) ($PhNH_2$/ODA)/PMDA co-PI films cured at 200 °C and (b) ($SPMNH_2$/ODA)/PMDA co-PI films cured at 200 °C and trend of different IDs of (c) ($PhNH_2$/ODA)/PMDA co-PI films cured at 200 °C and (d) ($SPMNH_2$/ODA)/PMDA co-PI films cured at 200 °C.

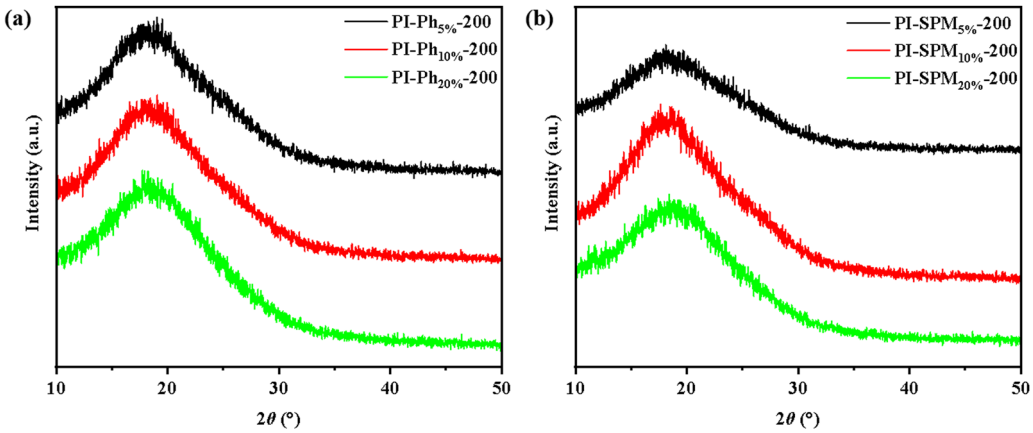

Fig. 3 XRD patterns of (a) ($PhNH_2$/ODA)/PMDA co-PI films cured at 200 °C and (b) ($SPMNH_2$/ODA)/PMDA co-PI films cured at 200 °C.

Table 1 Detailed data of ID_{1380}, *d*-spacing, CTE and dichroic ratios of the resulting PI films cured at 200 °C

Sample name	ID_{1380} (%)	*d*-Spacing (Å)	CTE (ppm K^{-1})	Dichroic ratio	Diamine ratio (*n*)
PI-200	86.9	4.67	26	2.36	ODA
PI-$Ph_{5\%}$-200	96.8	4.82	27	2.17	ODA : $PhNH_2$ = 9.5 : 0.5
PI-$Ph_{10\%}$-200	95.1	4.82	27	2.13	ODA : $PhNH_2$ = 9.0 : 1.0
PI-$Ph_{20\%}$-200	93.6	4.87	38	2.09	ODA : $PhNH_2$ = 8.0 : 2.0
PI-$SPM_{5\%}$-200	95.6	4.79	27	2.13	ODA : $SPMNH_2$ = 9.5 : 0.5
PI-$SPM_{10\%}$-200	98.3	4.82	29	2.10	ODA : $SPMNH_2$ = 9.0 : 1.0
PI-$SPM_{20\%}$-200	96.5	4.82	29	2.09	ODA : $SPMNH_2$ = 8.0 : 2.0

contain bulky side groups, the *d*-spacing values of ($PMNH_2$/ODA)/PMDA co-PI films were higher than those of the corresponding ($SPMNH_2$/ODA)/PMDA co-PI films. This result demonstrated that the pyrimidine side group endowed co-PI films with stronger intermolecular forces, and played a positive role in lowering the curing temperature.

Thermal properties

To gain insight into the dimensional stability of PI films, the coefficient of thermal expansion (CTE) values were tested by TMA, and the curves are illustrated in Fig. 4 and Fig. S12 (ESI†).[31,32] Compared to PI-200, the CTE of co-PI films increased from 27 ppm K^{-1} to 38 ppm K^{-1} with the addition of $PhNH_2$ due to gradually increased free volume and disturbed arrangement of molecular chains. However, for ($SPMNH_2$/ODA)/PMDA co-PI films, the values of CTE were maintained at around 29 ppm K^{-1} even when the amount of $SPMNH_2$ reached 20%, which suggested that the electrostatic interactions of the pyrimidine ring neutralised the negative effect of the bulky side group partly on CTE values.[33–35] The CTE value is closely related to the in-plane orientation of molecular chains as previously reported.[36] Therefore, we characterized in-plane orientation of the PI films by linearly polarized IR spectroscopy and calculated the dichroic ratio (*R*) to further estimate the arrangement of molecules (see Fig. S13 and S14, ESI†). *R* was evaluated from the absorbance area of IR at angles of polarization 0°, 90° and 180° according to the reported method.[37,38] With the addition of diamines containing bulky side groups, the *R* values of ($PhNH_2$/ODA)/PMDA co-PI films tended to decrease rapidly, while the *R* values changed slightly for $SPMNH_2$ based PI films. Therefore, the results of in-plane orientation of PI films matched well with the variation of CTE. The thermal stability including the thermal degradation temperatures of 5% and 10% ($T_{d5\%}$ and $T_{d10\%}$) were measured by TGA in a nitrogen atmosphere and are shown in Fig. 4, Fig. S15, Table 2 and Table S3 (ESI†). The $T_{d5\%}$ of all co-PI films was beyond 500 °C, and much higher than that of PI-200 (420 °C), which could be credited to the highly improved ID. For ($PhNH_2$/ODA)/PMDA co-PI films, the $T_{d5\%}$ values showed a gradual increasing trend from 507 to 530 °C with an increase in $PhNH_2$ due to the increase in the benzene ring content. Moreover, ($SPMNH_2$/ODA)/PMDA co-PI films exhibited higher $T_{d5\%}$ values compared to ($PMNH_2$/ODA)/PMDA co-PI films, which was in line with the stronger intermolecular interactions derived from the pyrimidine side group.[33–35,39,40]

Mechanical properties

The mechanical performances of PI films are a further criterion to evaluate the low temperature curing property. Besides, the significant improvement in the mechanical properties based on these low temperature curable co-PI films was one of the highlights of this work. The Young's modulus (*E*) and elongation at break (ε_b) of the PI films were improved apparently with the addition of $PhNH_2$ or $SPMNH_2$, which could be explained by the higher ID and toughening effect of side groups, as shown in Fig. 5, Fig. S16, Table 2 and Table S3 (ESI†). In addition, the

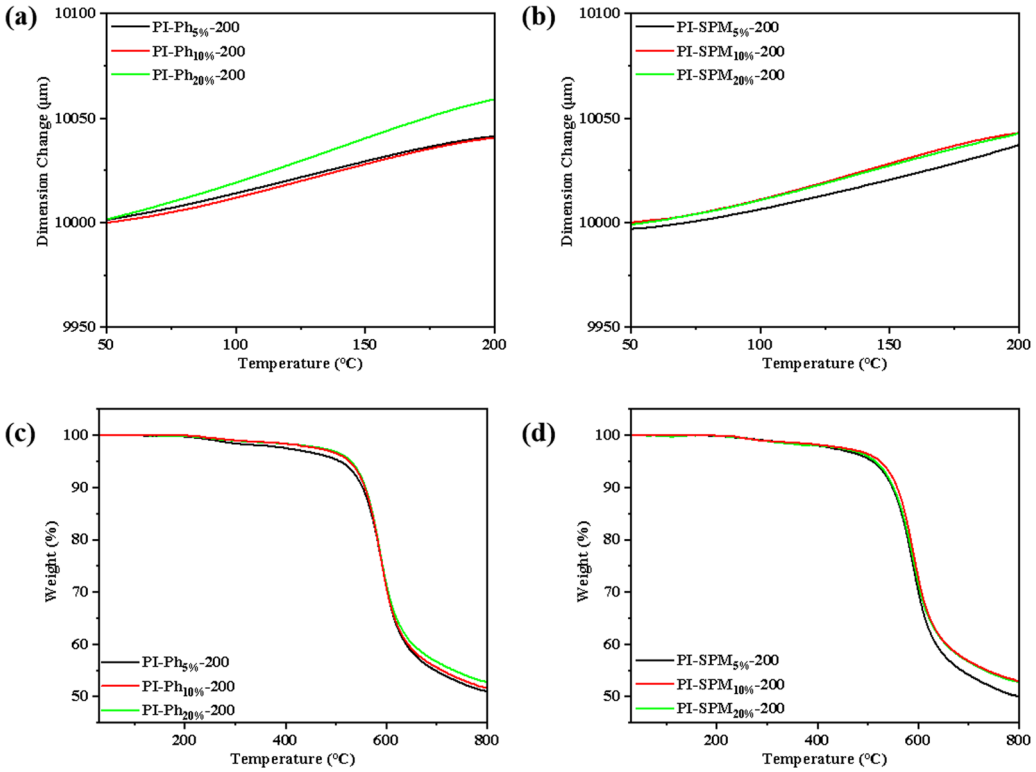

Fig. 4 TMA curves of (a) ($PhNH_2$/ODA)/PMDA co-PI films and (b) ($SPMNH_2$/ODA)/PMDA co-PI films; TGA curves of (c) ($PhNH_2$/ODA)/PMDA co-PI films and (d) ($SPMNH_2$/ODA)/PMDA co-PI films.

Table 2 Mechanical, thermal properties and other properties of the resulting PI films cured at 200 °C

	Thermal properties			Mechanical properties			Other properties		
	TGA		TMA	DMA					
Sample	$T_{d,5\%}$ [°C]	$T_{d,10\%}$ [°C]	T_g [°C]	σ_{max} [MPa]	ε_b [%]	E [GPa]	D_k [–]	D_f [%]	Contact angle [°]
PI-200	420	546	412	154	47.9	2.87	3.55	4.34	62.4
PI-$Ph_{5\%}$-200	507	552	361	131	54.8	2.89	3.41	2.39	72.5
PI-$Ph_{10\%}$-200	527	557	360	125	46.8	2.90	3.45	2.44	73.1
PI-$Ph_{20\%}$-200	530	559	344	119	72.4	2.99	3.40	2.13	77.8
PI-$SPM_{5\%}$-200	509	548	362	132	36.9	3.13	3.26	3.87	70.6
PI-$SPM_{10\%}$-200	524	558	359	147	103.4	3.20	3.42	4.91	69.9
PI-$SPM_{20\%}$-200	515	551	339	126	63.0	3.27	3.46	2.87	71.2

tensile strength (σ_{max}) of co-PI films was lower than that of PI-200 due to a higher degree of branching and increased distance of molecular chains, which coincided with the *d*-spacing values. It is worth noting that the σ_{max} of ($SPMNH_2$/ODA)/PMDA co-PI films was significantly less affected by the negative effects of the side groups than that of co-PI films with $PhNH_2$, owing to smaller *d*-spacing and more regular arrangement of co-PI molecular chains on introducing $SPMNH_2$. In particular, PI-$SPM_{10\%}$-200 exhibited outstanding mechanical properties among them, such as high Young's modulus (3.20 GPa), high tensile strength (147 MPa) and desirable elongation at break (103.4%), which was 116% higher than that of PI-200 and 54% higher than that of PI-350. As is well known, it was difficult achieve both high elongation at break and excellent tensile strength in low-temperature curable PI films, whereas $SPMNH_2$ helped achieve satisfactory mechanical properties due to the reasonable structure design. Except for this, both the thermal and mechanical properties of $SPMNH_2$ based low-temperature curable PI films showed the best performances among the reported PI films (as summarized in Table 3).

Theoretical calculations

To further evidence the catalytic activity in the polymerisation process, the chemical activity and alkalinity of the diamine monomer were investigated by theoretical calculation.[46,47] Herein, to further probe the relationship between the structures and the effects on lowering curing temperature, the pK_a

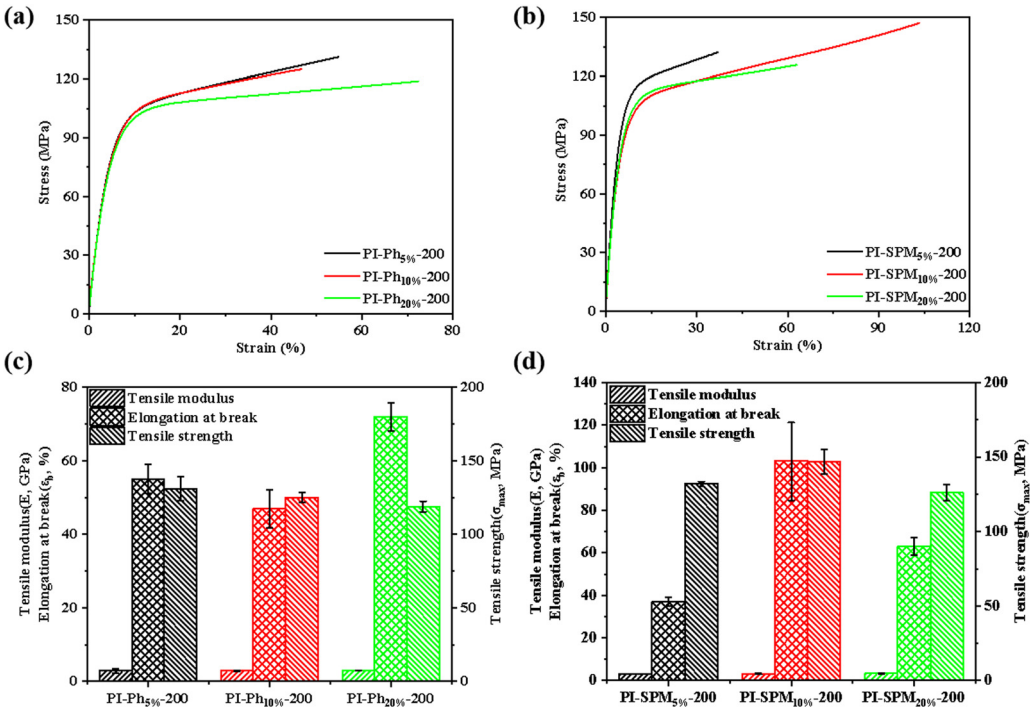

Fig. 5 Typical stress–strain curves of (a) ($PhNH_2$/ODA)/PMDA co-PI films and (b) ($SPMNH_2$/ODA)/PMDA co-PI films and detailed data of mechanical properties of (c) ($PhNH_2$/ODA)/PMDA co-PI films and (d) ($SPMNH_2$/ODA)/PMDA co-PI films.

Table 3 erformance of the reported low temperature curable PI films

	Thermal properties		Mechanical properties			Curing conditions		
	T_g	$T_{d,5\%}$	σ_{max}	ε_b	E	T_c		
Ref.	[°C]	[°C]	[MPa]	[%]	[GPa]	[°C]	Accelerator	Dosage
41	—	480	—	—	—	280	Et_3N	66.7%
42	225	510	—	—	—	220	QL	700%
13	289	592	112	75.5	1.27	200	QL	200%
12	—	545	134.82	145.16	1.66	200	QL	150%
12	—	456	105.40	45.37	1.01	200	IQL	150%
43	271	543	89	5.5	2.21	320	—	—
44	272	546.1	—	—	—	300	—	—
21	271	551	109	7.0	3.3	200	—	—
21	291	546	122	8.6	3.5	200	—	—
45	292	558	150	14.3	3.1	200	—	—
18	281	—	—	—	—	160	—	—
PI-$Ph_{20\%}$-200	344	530	119	72.4	2.99	200	—	—
PI-$SPM_{10\%}$-200	359	524	147	103.4	3.20	200	—	—

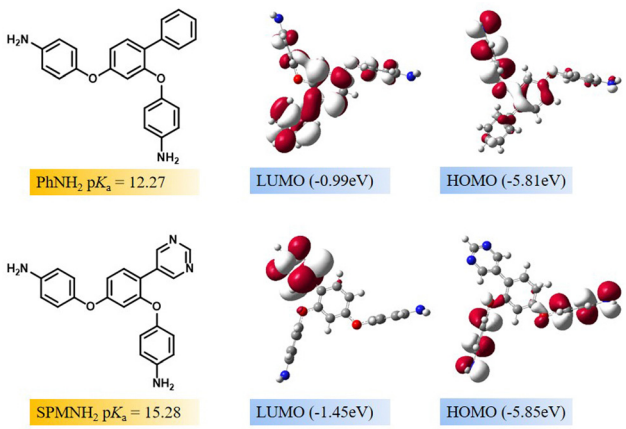

Fig. 6 Calculated pK_a values and HOMO/LUMO distributions of $PhNH_2$ and $SPMNH_2$.

values and electron-donating abilities of $PhNH_2$ and $SPMNH_2$ were evaluated according to the reported methods,[48,49] as shown in Fig. 6. First, the calculated pK_a values of $PhNH_2$ and $SPMNH_2$ were 12.27 and 15.28, respectively, which demonstrated that the alkalinity of $SPMNH_2$ was superior to that of $PhNH_2$ due to the presence of a pyrimidine ring, and it played a positive role in promoting the low-temperature curing ability as a base catalyst by decreasing the energy barrier. Second, the density functional theory (DFT) calculation results showed that $PhNH_2$ had shallower HOMOs (−5.81 eV) than $SPMNH_2$ (−5.85 eV), which could be attributed to the fact that the pyrimidine ring is a typical electron-withdrawing group. In addition, the dosage of $PhNH_2$ achieving the maximum ID in co-PI films was lower than that of $SPMNH_2$, which might be explained by the better reactivity of $PhNH_2$. Therefore, the alkalinity and electron-donating ability are two positive factors in promoting the imidization process, and needed to be considered in designing new diamines.

Electrical properties

With the rapid development of 5G communications, the electronic packaging materials with low dielectric constants (D_k)

and dielectric loss (D_f) at high frequency received increasing attention. Accordingly, the D_k of PI films was particularly associated with ID, polarizability and free volume of molecular chains.[50–52] The D_k and D_f values of the samples at 10 GHz were tested and are shown in Table 2 and Table S4 (ESI†). For PI-SPM$_x$-200 (X = 5%, 10% or 20%), the D_k values were in the range of 3.26 to 3.46. In particular, PI-SPM$_{5\%}$-200 (D_k = 3.26) had the lowest D_k among the PI films cured at 200 °C, due to the increased free volume and ID compared to that of PI-200. However, when the amount of SPMNH$_2$ was up to 20 wt%, the D_k of (SPMNH$_2$/ODA)/PMDA co-PI films increased rapidly, which could be attributed to the polarity of the pyrimidine ring. In addition, all low-temperature curable co-PI films showed D_f below 0.05, which was far from being applicable, and would be further reduced in our following work. The water contact angles of the PI films cured at 200 °C are listed in Table 2. Obviously, the addition of PhNH$_2$ or SPMNH$_2$ was beneficial to increase the water contact angles of the PI films due to the decrease in residual polar groups owing to improved IDs.

Experimental section

Preparation of ODA/PMDA PI films

10 mmol (2.0024 g) of ODA and 24 mL of DMAc were added into a three-necked flask in turn, followed by continuous mechanical stirring under nitrogen at room temperature until ODA was completely dissolved. After that, 10.00 mmol (2.1812 g) of PMDA was slowly added into the above solution in two parts and the solid content of reaction solution was maintained at 15%. Then, the PAA solution named PAA-0 was spin-coated on a clean glass after sufficiently stirring for 20 h and degassing. Next, the PI films underwent different thermal curing processes. And, 200 °C and 350 °C were chosen as their final curing temperatures, named PI-200 and PI-350. The heating process of PI films was as follows: the heating speed was 5 °C min^{-1} and maintained at 100 °C for 1 h, 200 °C for 1 h, 300 °C for 1 h, and 350 °C for 1 h, or 100 °C for 1 h and 200 °C for 3 h, respectively.

Preparation of (PhNH$_2$/ODA)/PMDA and (SPMNH$_2$/ODA)/PMDA co-PI films

To investigate the effect of side groups on lowering the curing temperature and obtain PI films with excellent properties, a series of co-PI films based on ODA and PMDA system copolymerization with new diamines were prepared. The PAAs were synthesized with different ratios of PhNH$_2$ or SPMNH$_2$ to the total molar amount of diamines, 5%, 10% and 20%, and the prepared films were named PI-Ph$_x$-y or PI-SPM$_x$-y, where x indicated the ratio given above and y represented the final curing temperature. The co-PI films of PMNH$_2$ were prepared as a contrast group and cured by the same procedure as PhNH$_2$ and SPMNH$_2$.

Conclusions

The introduction of nitrogen heterocycles is an advantageous method for the preparation of low-temperature curable polyimide. Herein, the effect of substitution sites of nitrogen heterocycles on low-temperature curing ability was investigated by comparing three different diamine structures. The introduction of a suitable amount of bulky side groups in polyimide can affect molecular chain alignment, thus exerting a certain low-temperature curing effect in the absence of nitrogen heterocycles. We have also proposed the possibility that the pyrimidine side group has better low-temperature curing ability and could substantially improve the mechanical and thermal properties of low-temperature curable polyimide compared to when the pyrimidine ring is placed in the main chain. The novel diamine structure with a pyrimidine side group has enabled us to obtain low-temperature curable polyimide with an ID of 98.3%. Meanwhile, PI-SPM$_{10\%}$-200 exhibited excellent mechanical and thermal properties among all the prepared co-PI films (Young's modulus of 3.20 GPa, an elongation of 103.4%, a tensile strength of 147 MPa, a $T_{d5\%}$ of 524 °C, a T_g of 359 °C and a CTE of 29 ppm K^{-1}). We expect that this contribution will further enrich design strategies for low-temperature curable structures and provide a highly promising PI material applied in the fan-out wafer level package industry and other fields.

Conflicts of interest

There are no conflicts to declare.

Acknowledgements

This work was financially supported by National Natural Science Foundation of China (61904191 and 62174170), the Key R&D Project of Guangdong Province (2020B010180001), Guangdong Joint Funding (2020A1515110934), the Key Laboratory of Guangdong Province (2014B030301014), the SIAT Innovation Program for Excellent Young Researchers (E2G030), and the National Key R&D Project from Minister of Science and Technology of China (2017ZX02519).

Notes and references

1 Z. Cheng, Y. Ding, L. Xiao, X. Wang and Z. Chen, *Microelectron. Reliab.*, 2019, **103**, 113512.
2 L. Bu, S. Ho, S. D. Velez, T. Chai and X. Zhang, *IEEE Trans.*, 2013, **3**(10), 1647–1653.
3 B. Chen, X. Li, Y. Jia, J. Yang and C. Li, *Polym. Compos.*, 2018, **39**, 1626–1634.
4 J. W. Baek, W. S. Yang, M. J. Hur, J. C. Yun and S. J. Park, *Mater. Sci. Semicond. Process.*, 2019, **91**, 392–398.
5 D. J. Liaw, K. L. Wang, Y. C. Huang, K. R. Lee, J. Y. Lai and C. S. Ha, *Prog. Polym. Sci.*, 2012, **37**(7), 907–974.
6 I. Gouzman, E. Grossman, R. Verker, N. Atar, A. Bolker and N. Eliaz, *Adv. Mater.*, 2019, **31**(18), 1807738.
7 M. Kaltenbrunner, T. Sekitani, J. Reeder, T. Yokota, K. Kuribara, T. Tokuhara, M. Drack, R. Schwodiauer and I. Graz, *Nature*, 2013, **499**(7459), 458–463.

8 C. H. Lee, B. Huang, J. See, L. Prenger, Y. M. Lin and W. L. Chiu, *IEEE Trans.*, 2022, **12**(4), 692–699.
9 R. J. Iredale, C. Ward and I. Hamerton, *Prog. Polym. Sci.*, 2017, **69**, 1–21.
10 T. Sasaki, *J. Photopolym. Sci. Technol.*, 2016, **29**(3), 379–382.
11 J. Kusunoki and T. Hirano, *J. Photopolym. Sci. Technol.*, 2005, **18**(2), 321–325.
12 C. Huang, J. Li, D. Sun, R. Xuan, Y. Sui and T. Li, *J. Mater. Chem. C*, 2020, **8**(42), 14886–14894.
13 Y. Ding, B. Bikson and J. K. Nelson, *Macromolecules*, 2002, **35**(3), 905–911.
14 A. A. Kuznetsov, *High Perform. Polym.*, 2000, **12**(3), 445–460.
15 K. S. Jang, D. Wee, Y. H. Kim, J. Kim, T. Ahn and J. W. Ka, *Langmuir*, 2013, **29**(23), 7143–7150.
16 T. S. Leu and C. S. Wang, *J. Polym. Sci., Part A: Polym. Chem.*, 2001, **39**, 4139–4151.
17 Y. Zhuang, J. G. Seong and Y. M. Lee, *Prog. Polym. Sci.*, 2019, **92**, 35–88.
18 X. Han, Y. Tian, L. Wang, C. Xiao and B. Liu, *Eur. Polym. J.*, 2007, **43**(10), 4382–4388.
19 X. Li, P. Zhang, J. Dong, F. Gan and X. Zhao, *Composites, Part B*, 2019, **177**, 107401.
20 V. N. Artem'eva, V. V. Kudryavtsev, E. M. Nekrasova and V. P. Sklizkova, *Russ. Chem. Bull.*, 1994, **43**(3), 387–390.
21 C. Li, Y. Wang, Y. Yin, Y. Li and J. Li, *Polymer*, 2021, **228**, 123963.
22 Y. Sui, J. Li, T. Wang, D. Sun and C. Huang, *Polymer*, 2021, **218**, 123514.
23 K. Fukukawa and M. Ueda, *Polym. J.*, 2006, **38**(5), 405–418.
24 M. Hu, H. Chen, M. Wang, G. Liu, C. Chen and G. Qian, *J. Polym. Sci.*, 2021, **59**(4), 329–339.
25 X. Lv, S. Qiu, S. Huang, K. Wang and J. Li, *Polymer*, 2022, **261**, 125418.
26 X. Jin and D. Zhu, *Eur. Polym. J.*, 2008, **44**(11), 3571–3577.
27 C. A. Pryde, *J. Polym. Sci., Part A: Polym. Chem.*, 1993, **31**, 1045–1052.
28 Y. Zhai, Q. Yang, R. Zhu and Y. Gu, *J. Mater. Sci.*, 2008, **43**(1), 338–344.
29 Q. Wu, X. Ma, F. Zheng, X. Lu and Q. Lu, *Eur. Polym. J.*, 2019, **120**, 109235.
30 L. Yi, W. Huang and D. Yan, *J. Polym. Sci., Part A: Polym. Chem.*, 2017, **55**(4), 533–559.
31 K. Seo, K.-H. Nam, S. Lee and H. Han, *Mater. Lett.*, 2020, **263**, 127204.
32 K.-H. Nam, S. Kim, J. Song, S. Baek and S.-H. Paek, *Macromol. Res.*, 2016, **24**(2), 104–113.
33 V. M. Nazarychev, S. V. Larin, A. V. Yakimansky, N. V. Lukasheva and A. A. Gurtovenko, *J. Polym. Sci., Part B: Polym. Phys.*, 2015, **53**(13), 912–923.
34 V. M. Nazarychev, A. V. Lyulin, S. V. Larin, I. V. Gofman, J. M. Kenny and S. V. Lyulin, *Macromolecules*, 2016, **49**(17), 6700–6710.
35 S. V. Lyulin, S. V. Larin, A. A. Gurtovenko, N. V. Lukasheva, V. E. Yudin, V. M. Svetlichnyi and A. V. Lyulin, *Polym. Sci., Ser. A*, 2012, **54**, 631–643.
36 J. H. Jou and P. T. Huang, *Macromolecules*, 1991, **24**(13), 3796–3803.
37 S. I. Matsuda and S. J. Ando, *J. Polym. Sci., Part B: Polym. Phys.*, 2003, **41**(4), 418–428.
38 Y. Y. Tian, L. B. Luo, Q. Q. Yang, L. J. Zhang, M. Wang, D. F. Wu, X. Wang and X. Y. Liu, *Polymer*, 2020, **188**, 122100.
39 Z. Yang, P. Ma, F. Li, H. Guo, C. Kang and L. Gao, *Eur. Polym. J.*, 2021, **148**, 110369.
40 F. Tong, Z. Chen, X. Lu and Q. Lu, *J. Mater. Chem. C*, 2017, **5**(39), 10375–10382.
41 W. H. Liao, S. Y. Yang, S. T. Hsiao, Y. S. Wang, S. M. Li, C. C. Ma, H. W. Tien and S. J. Zeng, *ACS Appl. Mater. Interfaces*, 2014, **6**(18), 15802–15812.
42 R. Lian, X. Lei, Y. Chen and Q. Zhang, *J. Appl. Polym. Sci.*, 2019, **136**(31), 47771.
43 J. O. Simpson and A. K. Clair, *Thin Solid Films*, 1997, **308**, 480–485.
44 X. Liu, X. W. Cao, G. J. He and T. C. Xing, *eXPRESS Polym. Lett.*, 2019, **13**(6), 524–532.
45 C. Li, G. Zhang, J. Li and Y. Sui, 22nd International Conference on Electronic Packaging Technology, ICEPT 2021.
46 M. M. Koton, V. N. Artemeva, V. V. Kudryavtsev, Z. D. Chernova, N. V. Kukarkina, L. A. Ovsyannikova and G. D. Rudkovskaya, *Vysokomol. Soedin., Ser. A*, 1983, **25**(4), 726–731.
47 V. M. Svetlichnyi, N. G. Antonov, B. V. Chernitsa, V. M. Denisov, A. I. Koltsov, V. V. Kudryavtsev and M. M. Koton, *Vysokomol. Soedin., Ser. A*, 1986, **28**(11), 2412–2418.
48 S. Miertuš and J. Tomasi, *Chem. Phys.*, 1981, **55**, 117–129.
49 F. Weigend, *Phys. Chem. Chem. Phys.*, 2005, **7**, 3297–3305.
50 T. Matsuura, Y. Hasuda, S. Nishi and N. Yamada, *Macromolecules*, 1991, **24**(18), 5001–5005.
51 Y. Li, G. Sun, Y. Zhou, G. Liu, J. Wang and S. Han, *Prog. Org. Coat.*, 2022, **172**, 107103.
52 R. Bei, C. Qian, Y. Zhang, Z. Chi, S. Liu, X. Chen and J. Xu, *J. Mater. Chem. C*, 2017, **5**(48), 12807–12815.

